Control of energy dissipation between a periodically driven Hubbard model and a fermionic bath

Tel Aviv University

11/09/2018

Introduction

Strongly correlated materials.

- Idea of description of electrons in solids as independent particles
  $\rightarrow$ wave-like picture
- Materials in which electrons tend to *localize*
  $\rightarrow$particle-like picture
- Strong electronic correlations brings out a variety of phenomena, e.g. metal-to-Mott-insulator transitions

Description of the lattice

Hubbard model.

$$H_{\text{Hubbard}} = -\sum_{\langle i,j\rangle,\sigma} v_{ij} d^{\dagger}_{i\sigma} d_{j\sigma} + \sum_{i} U(d^{\dagger}_{i\uparrow} d_{i\uparrow} - \frac{1}{2})(d^{\dagger}_{i\downarrow} d_{i\downarrow} - \frac{1}{2})$$

- $\mathrm{v_{ij}} \simeq$ overlap between orbitals on neighboring atomic sites $\sim \mathrm{eV}$
- Coulomb repulsion U, screened value $\sim \mathrm{eV}$

$\rightarrow$ competition between energy scales

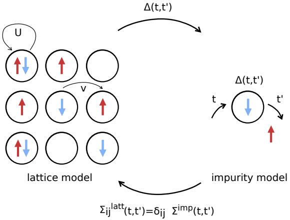

Figure (1): Lattice model

Dynamical Mean Field Theory

Idea of mapping.

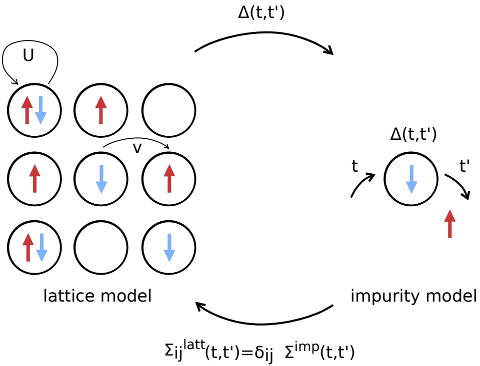

Figure (2): Mapping of the lattice problem onto an Impurity problem

- Approximate lattice problem with many degrees of freedom by *single-site problem*

Dynamical Mean Field Theory

Set of self-consistent equations.

- compute local Greens function $G^{\sigma}_{ii}(t-t') = -i\langle \mathscr{T} d_{i\sigma}(t) d^{\dagger}_{i\sigma}(t')\rangle$ from an effective impurity model with action

$$S = i\int_C dt U n_{\uparrow}(t) n_{\downarrow}(t) - i\sum_{\sigma}\int_C dt dt' d^{\dagger}_{\sigma}(t)\Delta(t-t') d_{\sigma}(t')$$

- use impurity self energy, defined via $G^{-1}_{ii}(\omega) = \omega + \mu - \Delta(\omega) - \Sigma^{imp}(\omega)$, to obtain the lattice Greens function

$$G^{-1}_{ij}(\omega) = \delta_{ij}[\omega + \mu - \Sigma_{ii}(\omega)] - v_{ij}$$

$$\Sigma_{ii}(\omega) \simeq \Sigma^{imp}(\omega); \Sigma_{i\neq j}(\omega) \simeq 0$$

- average over the Brillouin zone to get the on-site component:

$$G_{ii}(\omega) = \frac{1}{L}\sum_k G_k(\omega) = \frac{1}{L}\sum_k \frac{1}{\omega + \mu + \Sigma(\omega) - \varepsilon_k}$$

Dynamical Mean Field Theory

Set of self-consistent equations.

$$G_0 = \omega + \mu - \Delta(\omega)$$

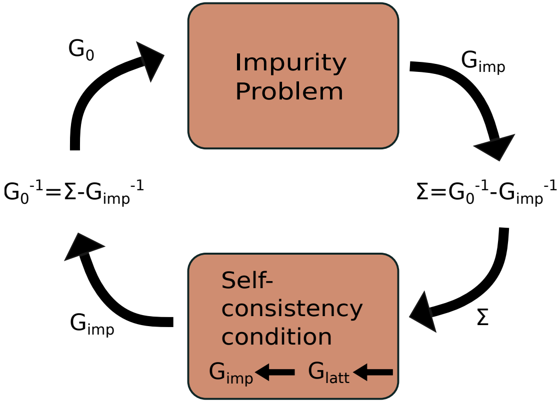

Figure (3): DMFT iterative loop

Real Time Impurity Solver

Pertubative expansion.

Single-orbital Anderson impurity model $H_{\text{imp}} = H_{\text{loc}} + H_{\text{bath}} + H_{hyb}$:

$$H_{\text{loc}} = \sum_{\sigma\in\uparrow,\downarrow} \varepsilon_\sigma d^\dagger_\sigma d_\sigma + U n_\uparrow n_\downarrow$$

$$H_{\text{bath}} = \sum_{\sigma,\lambda} \varepsilon_\lambda b^\dagger_\lambda b_\lambda$$

$$H_{\text{hyb}} = \sum_{\sigma,\lambda} (t_{\sigma\lambda} b^\dagger_\lambda d_\sigma + t^*_{\sigma\lambda} d^\dagger_\sigma b_\lambda)$$

- Write impurity Hamiltonian as a sum $H_{\text{imp}} = H_0 + H_{\text{int}}$
- Exact time evolution for H_0, pertubative expansion for H_{int}

Real Time Impurity Solver

Calculation of expectation values.

- Goal is to evaluate objects like $G^{<}(t,t') = i\langle d^{\dagger}(t')d(t)\rangle$ and $G^{>}(t,t') = -i\langle d(t)d^{\dagger}(t')\rangle$
- Expectation values are given by $\langle O(t)\rangle = Tr\left(\rho U^{\dagger}(t)\hat{O}U(t)\right)$
- Interaction picture propagator $U(t) = \exp^{iH_0t}\exp^{-iHt}$ and operator $\hat{O}(t) = \exp^{iH_0t} O \exp^{-iH_0t}$
- Reduced Hamiltonian $H_0 = H_{\text{imp}} - H_{\text{hyb}}$

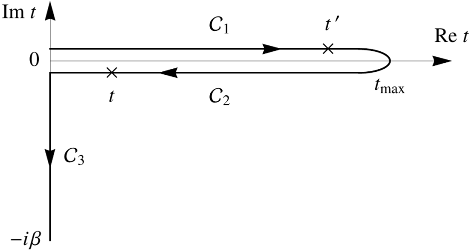

Figure (4): Keldysh Contour

Real Time Impurity Solver

Hybridization expansion.

- Expansion of $U(t)$ and $U^\dagger(t)$ in terms of $\widehat{H}_{\text{hyb}}$:

$$U(t) = \sum_{n=0}^{\infty} (-i)^n \int_0^t dt_1 \int_0^{t_1} dt_2 \cdots \int_0^{t_{n-1}} dt_n \widehat{H}_{\text{hyb}}(t_1)\widehat{H}_{\text{hyb}}(t_2)\cdots\widehat{H}_{\text{hyb}}(t_n)$$

- Insert expansion for U(t) into propagator between many body states:

$$G(t) = \langle\langle\alpha \mid \rho_D exp^{-iHt} \mid \beta\rangle\rangle_B = \langle\langle\alpha \mid \rho_D \exp^{-iH_0 t} U(t) \mid \beta\rangle\rangle_B$$

- many body states are $|0\rangle, |\uparrow\rangle, |\downarrow\rangle, |\uparrow\downarrow\rangle$
- $\langle\cdots\rangle_B = Tr\{\rho_B \cdots\}$

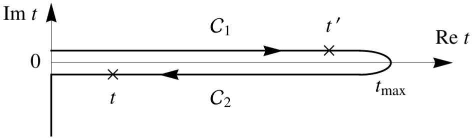

Figure (5): Keldysh Contour

Real Time Impurity Solver

Hybridization expansion.

$$G_{\alpha\alpha}(t) = G^{(0)}_{\alpha\alpha}(t) - \sum_{\gamma\delta} \int_0^t dt_1 \int_0^{t_1} dt_2 G^{(0)}_{\alpha\alpha}(t-t_1) G^{(0)}_{\beta\beta}(t_1-t_2) \Delta^{\gamma\delta}_{\alpha\beta}(t_1-t_2) G^{(0)}_{\alpha\alpha}(t_2) - \cdots$$

with bare propagators

$$G^{(0)}_{\alpha\alpha}(t) = \langle\langle \alpha \mid \rho_D \exp^{-iH_0 t} \mid \alpha\rangle\rangle_B = \exp^{-i\varepsilon_\alpha t}$$

and Hybridization

$$\begin{aligned} \Delta(t_1-t_2) = \langle \alpha \mid d_\sigma \mid \beta\rangle\langle\beta \mid d^\dagger_\sigma \mid \alpha\rangle \Delta^<(t_1-t_2) + \\ \langle \alpha \mid d^\dagger_\sigma \mid \beta\rangle\langle\beta \mid d_\sigma \mid \alpha\rangle \Delta^>(t_1-t_2) \end{aligned}$$

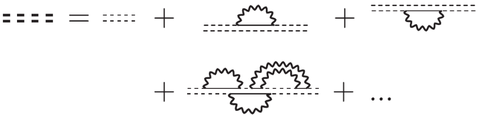

Real Time Impurity Solver

Hybridization expansion.

Dyson equation:

$$G_{\alpha\alpha}(t) = G^{(0)}_{\alpha\alpha}(t) + \int_0^t dt_1 \int_0^{t_1} dt_2 G^{(0)}_{\alpha\alpha}(t-t_1)\Sigma_{\alpha\alpha}(t_1-t_2)G_{\alpha\alpha}(t_2)$$

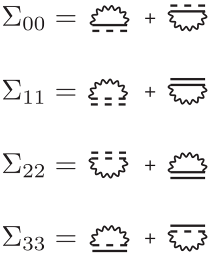

Figure (7): NCA Self-energy

Self-consistent solution

1. Initialize $G_{\alpha\alpha}(t)$ with $G^{(0)}_{\alpha\alpha}(t)$
2. Compute self-energy $\Sigma_{\alpha\alpha}(\mathrm{t})$
3. Update $G_{\alpha\alpha}(t)$
4. go back to step 2

source: G. Cohen, D. R. Reichman, A. J. M. and E. Gull; Phys. Rev. B89, 112139(2014)

Vertex functions:

$$K_{\alpha\beta}(t,t') = K^{(0)}_{\alpha\beta}(t,t') + \sum_{\gamma\delta} \int_0^t dt_1 \int_0^{t'} dt_2 K_{\alpha\gamma}(t_1,t_2)\Delta_{\gamma\delta}(t_1,t_2) G^{\dagger}_{\delta\beta}(t-t_1) G_{\delta\beta}(t'-t_2)$$

$$K^{(0)}_{\alpha\beta}(t,t') = G^{\dagger}_{\alpha\beta}(t) G_{\alpha\beta}(t')$$

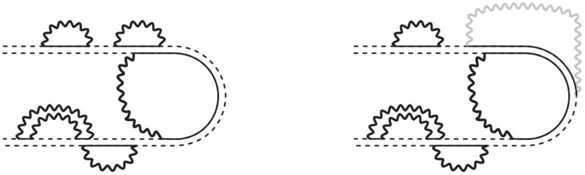

Figure (8): Diagrammatic expansion for Vertex functions

Driven System

Bethe lattice in the initial Neel state.

Self-consistency condition:

$$\Delta_{A(B),\sigma}(t,t') = v(t) G_{B(A),\sigma}(t,t') v^*(t')$$

Time-dependent electric field:

$$H_{\mathrm{drv}}(t) = \sum_j eaE_0 sin(\omega t) s_j n_j$$

$$v_{ij}(t) = v_{ij} e^{iA(s_i - s_j) cos(\omega t)}$$

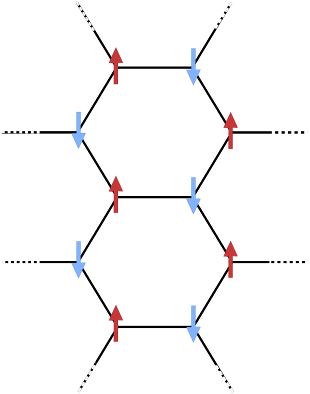

Figure (9): Structure of an anti-ferromagnetic lattice

Extension to an Open System

Free-fermion bath

$$H_{\text{tot}} = H_{\text{imp}} + H_{\text{fBath}} + H_{\text{fMix}}$$

$$H_{\text{fBath}} = \sum_{k,\sigma} \varepsilon_k f^\dagger_{k,\sigma} f_{k,\sigma}$$

$$H_{\text{fMix}} = \sum_{k,\sigma} (V_k f^\dagger_{k,\sigma} d_\sigma + V^*_k d^\dagger_\sigma f_{k,\sigma})$$

$$G(t,t') = (G_0^{-1}(t,t') - \Sigma_{\text{fBath}}(t,t') - \Sigma(t,t'))^{-1}$$

Figure (10): Schematic representation of a free-fermion bath model

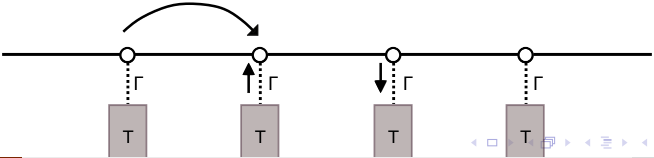

Schrieffer-Wolff Transformation

to the periodically driven Fermi-Hubbard model with $v_0 \ll U, \omega$

Transformation to the rotating frame with $V(t) = e^{-iUt\sum_j n_{j\uparrow}n_{j\downarrow} + \sum_{j,\sigma} F_{j,\sigma}(t) n_{j,\sigma}}$:

$$
\begin{aligned}
H &= -v_0 \sum_{\langle i,j\rangle,\sigma}^{N} d^\dagger_{i\sigma} d_{j\sigma} + U \sum_{j}^{N} n_{j\uparrow} n_{j\downarrow} + \sum_{j,\sigma} f_{j,\sigma}(t) n_{j,\sigma} \\
&\Downarrow \\
H^{\mathrm{rot}}(t) &= -v_0 \sum_{<i,j>,\sigma} [e^{i\delta F_{ij\sigma}(t)} g_{ij\sigma} + (e^{i\left[Ut + \delta F_{ij\sigma}(t)\right]} h^\dagger_{ij\sigma} + h.c.)]
\end{aligned}
$$

$$
\begin{aligned}
h^\dagger_{ij\sigma} &= n_{i\bar\sigma} d^\dagger_{i\sigma} d_{j\sigma} (1 - n_{j\bar\sigma}) \\
g_{ij\sigma} &= (1 - n_{i\bar\sigma}) d^\dagger_{i\sigma} d_{j\sigma} (1 - n_{j\bar\sigma}) + n_{i\bar\sigma} d^\dagger_{i\sigma} d_{j\sigma} n_{j\bar\sigma}
\end{aligned}
$$

Schrieffer-Wolff Transformation

to the periodically driven Fermi-Hubbard model with $v_0 \ll U, \omega$

doublon and holon hopping $g_{ij\sigma} = (1 - n_{i\bar{\sigma}}) d^\dagger_{i\sigma} d_{j\sigma} (1 - n_{j\bar{\sigma}}) + n_{i\bar{\sigma}} d^\dagger_{i\sigma} d_{j\sigma} n_{j\bar{\sigma}}$:

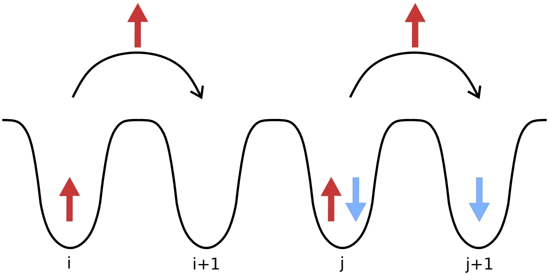

doublon and holon creation $h^{\dagger}_{ij\sigma} = n_{i\bar{\sigma}} d^{\dagger}_{i\sigma} d_{j\sigma} (1 - n_{j\bar{\sigma}})$:

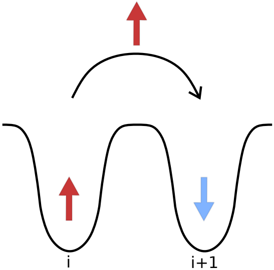

Schrieffer-Wolff Transformation

for the resonantly driven Fermi-Hubbard model with $v_0 \ll U = l\omega$

Leading order term of time-periodic Hamiltonian $H(t+T) = H(t)$:

$$
\begin{aligned}
H_{\text{eff}}^{(0)} &= \frac{1}{T}\int_0^T dt H^{\text{rot}}(t) \\
&= -\frac{1}{T}\int_0^T dt \sum_{<i,j>,\sigma} v_0 [e^{i\delta F_{ij\sigma}(t)} g_{ij\sigma} + (e^{i\left[Ut+\delta F_{ij\sigma}(t)\right]} h^{\dagger}_{ij\sigma} + h.c.)] \\
&= \sum_{<i,j>,\sigma} \left\{ -J_{\text{eff}} g_{ij\sigma} - K_{\text{eff}} \left[(-1)^l h^{\dagger}_{ij\sigma} + h.c. \right] \right\}
\end{aligned}
$$

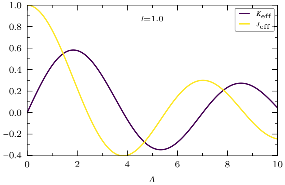

Effective Tunneling Rate

of the dissipative, driven Fermi-Hubbard model

$$H_{\mathrm{fMix}} = \sum_{j,k,\sigma} (V_k b^\dagger_{k,\sigma} d_{j,\sigma} + h.c.)$$

$$W = 2\pi \sum \rho \mid H_{\mathrm{fMix}} \mid^2$$

$$\Downarrow$$

transformation to the rotating frame, averaging over one period:

$$W^{(0)}_{\mathrm{eff}} = 2\pi \sum_{\langle i,j\rangle k,k',\sigma} \rho \left\{ J^{\mathrm{bath}}_{\mathrm{eff}} b^\dagger_{k,\sigma} b_{k',\sigma} g_{ij\sigma} + K^{\mathrm{bath}}_{\mathrm{eff}} ((-1)^l b^\dagger_{k,\sigma} b_{k',\sigma} h^\dagger_{ij\sigma} + h.c.) \right\}$$

Effective Tunneling Rate

of the dissipative, driven Fermi-Hubbard model

$$W_{\text{eff}}^{(0)} = 2\pi \sum_{\langle i,j\rangle k,k',\sigma} \rho \left\{ J_{\text{eff}}^{\text{bath}} b_{k,\sigma}^{\dagger} b_{k',\sigma} g_{ij\sigma} + K_{\text{eff}}^{\text{bath}} \left((-1)^{l} b_{k,\sigma}^{\dagger} b_{k',\sigma} h_{ij\sigma}^{\dagger} + h.c. \right) \right\}$$

$$\begin{aligned} K_{\text{eff}}^{\text{bath}} &= V_k V_{k'}^{*} \mathscr{J}_l(A) \\ J_{\text{eff}}^{\text{bath}} &= V_k V_{k'}^{*} \mathscr{J}_0(A) \end{aligned}$$

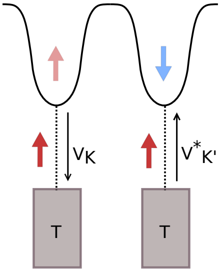

Results for a Mott Insulator

How does the system's ability to dissipate energy change out of equilibrium?

Energy current:

$$I_{\mathrm{E}}(t) = \langle \mathscr{I}_{\mathrm{E}}(t) \rangle$$

$$\mathscr{I}_{\mathrm{E}} = \dot{H}_{\mathrm{fBath}} = i \sum_{k,\sigma} \varepsilon_k (V_k d_\sigma f^\dagger_{k,\sigma} - V^*_k f_{k,\sigma} d^\dagger_\sigma)$$

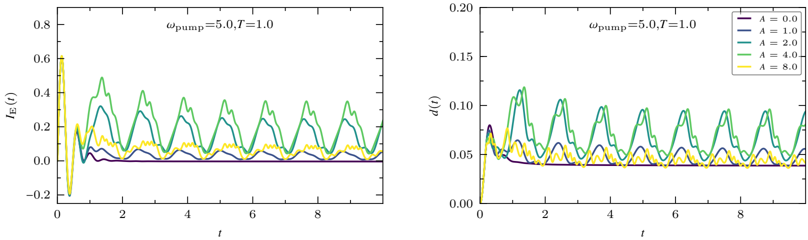

Figure (11): Time-dependent heat current (left) between the system with $U/t_0 = 10$ and the fermionic bath, induced by a resonant driving field at different field strengths and double occupation (right).

Results for a Mott Insulator

How does the system's ability to dissipate energy change out of equilibrium?

Time-averaged energy current:

$$\bar{I}_{\mathrm{E}}(t) = \frac{1}{T}\int_0^T ds I_{\mathrm{E}}(t, t-s)$$

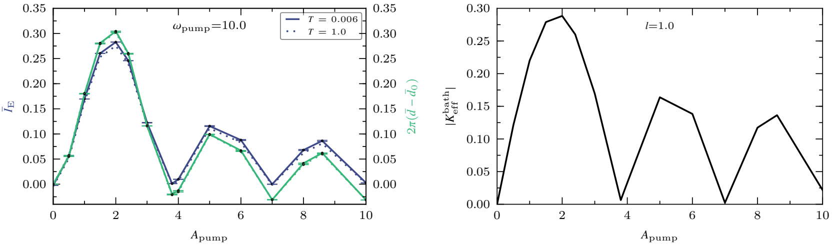

Figure (12): Left: Field-strength dependence of period averaged energy current $\bar{I}_E$ and normalized doublon density $\bar{d} = <\overline{n_\uparrow n_\downarrow}>$ in the $l = 1$ regime with $U = \omega_{\mathrm{pump}} = 10$. Right: Renormalized bath hopping parameter $K_{\mathrm{eff}}^{\mathrm{bath}}$ associated with the creation of doublons and holons.

How does the system's ability to dissipate energy change out of equilibrium?

Response function:

$$P_\omega(A_{\text{probe}}) = \lim_{A\to 0} \frac{dI_E(A_{\text{probe}}(\omega_{\text{probe}}))}{dA_{\text{probe}}(\omega_{\text{probe}})} \simeq \frac{I_{\text{E}}(\Delta A_{\text{probe}}(\omega_{\text{probe}}))}{\Delta A_{\text{probe}}(\omega_{\text{probe}})}$$

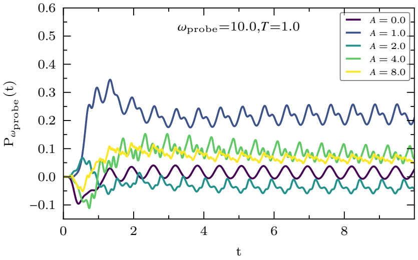

Figure (13): Time-dependent response of the energy current in a resonantly driven system with $U = \omega_{\text{pump}} = 10$.

Results for a Mott Insulator

Response of the heat current in equilibrium.

Period-averaged response function:

$$\overline{P}_{\omega_{\text{probe}}}(t) = \frac{1}{T}\int_0^T ds P_{\omega_{\text{probe}}}(t, t-s)$$

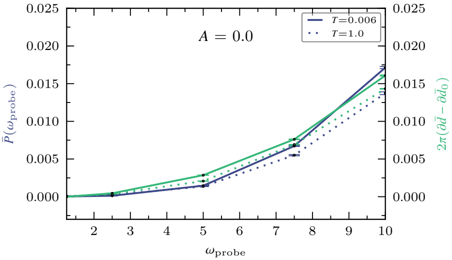

Figure (14): Averaged change of the energy flow $\overline{P}_E$ and double occupation $\partial\overline{d} = \frac{\overline{d}(\Delta A_{\text{probe}}(\omega_{\text{probe}}))}{\Delta A_{\text{probe}}(\omega_{\text{probe}})}$ generated by a probe pulse at different frequencies ω_{probe} for a gapped system in equilibrium.

Results for a Mott Insulator

Response of the heat current at resonant driving with $U/\omega_{pump} = 10$

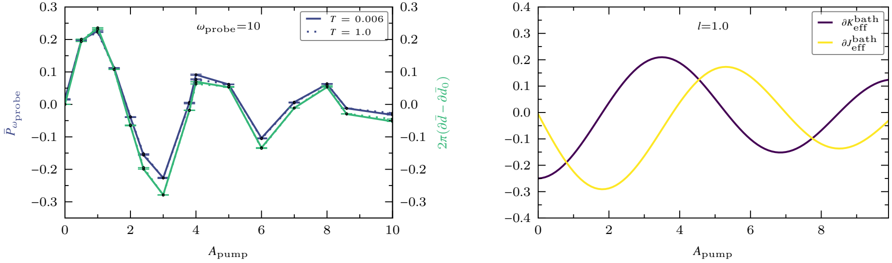

Figure (15): Left: Period-averaged response and double occupation $\partial_{A_{probe}}\bar{d}(A_{\rm pump})$ generated by a probe pulse at $\omega_{\rm probe} = 10$ as a function of the driving amplitude. Right: Change of doublon-holon creation parameter $K^{\rm bath}_{\rm eff}$ and hopping $J^{\rm bath}_{\rm eff}$ as a response to the probe field.

Results for a Mott Insulator

Nonequilibrium distribution functions.

$$F(\omega,t) = \frac{ImG^{<}(\omega,t)}{2\pi A(\omega,t)}$$

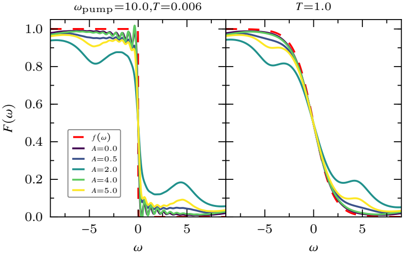

Figure (16): Nonequilibrium distribution functions of a Mott insulator in the resonant driving regime with $U = \omega_{\text{pump}} = 10$, coupled to a fermionic bath at $T = 0.006$ and $T = 1.0$. The red line corresponds to the Fermi-Dirac distribution.

Results for a Mott Insulator

Spectral properties for $U/v_0 = 10$.

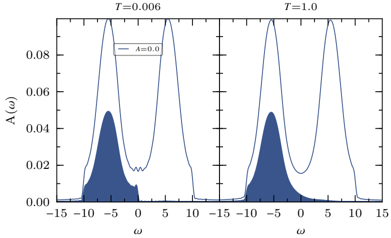

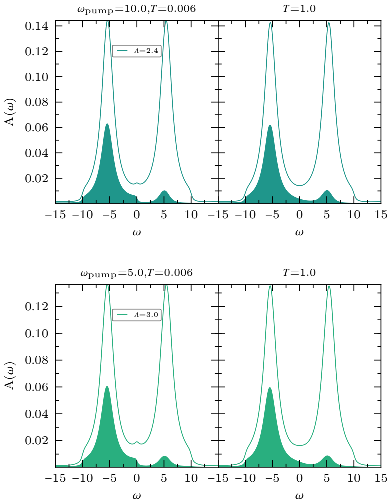

Figure (17): Left: Spectral function $A(\omega)$ (thick line) and occupation $N(\omega)$ (shaded region) for an undriven system. Right: Comparison to a resonantly driven system shows that specific driving amplitudes A induce an occupation inversion depending on the driving mechanism.

Results for a Mott-like System

Control of the energy current at $U/v_0 = 5$.

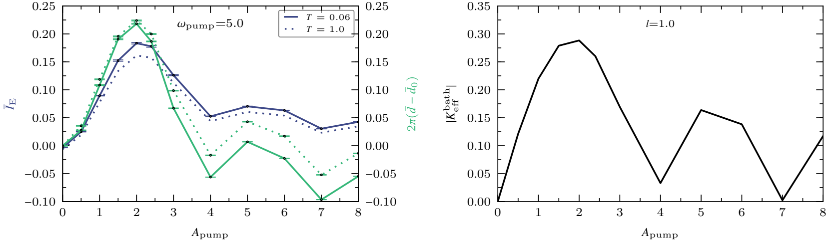

Figure (18): Left: Field-strength dependence of period averaged energy current $\bar{I}_E$ and normalized doublon density $\bar{d} = <\overline{n_\uparrow n_\downarrow}>$ in the $l = 1$ regime with $U = \omega_{\text{pump}} = 5$. Right: Renormalized bath hopping parameter $K_{\text{eff}}^{\text{bath}}$ associated with the creation of doublons and holons.

Results for a Mott-like System

Spectral properties for $U/v_0 = 5$.

$$A(\omega) = -\frac{1}{\pi} Im G^r(\omega) \text{ with } G^r(t,t') = \Theta(t-t')(G^>(t,t') - G^<(t,t'))$$

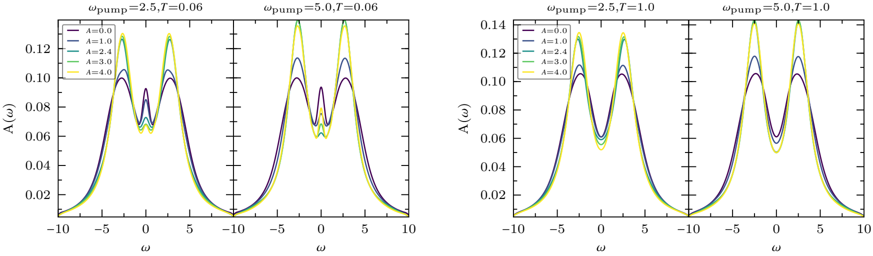

Figure (19): Period- and spin-averaged spectral functions for a bath temperature $T = 0.06$ and $T = 1.0$ in the two different driving regimes with increasing field amplitude. For $T \leq T_K$ the emergence of a Kondo peak can be controlled through the amplitude of the electric field.

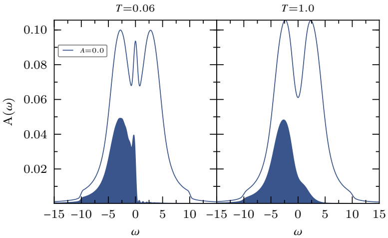

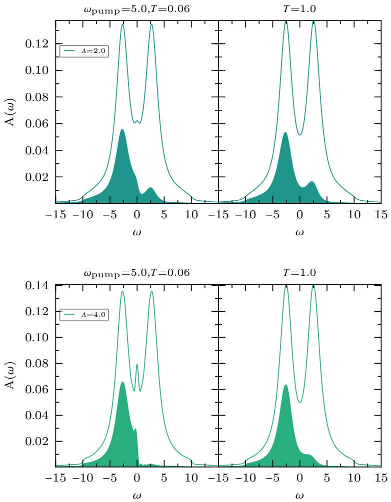

Figure (20): Left: Spectral function $A(\omega)$ (thick line) and occupation $N(\omega)$ (shaded region) for an undriven system. Right: Nonequilibrium spectral functions and occupations for amplitudes, which maximize (upper) or minimize (lower) the effective temperature and double occupation.

Summary

Resonant driving enables:

- a presice control of energy flow between a Mott insulator and its environment

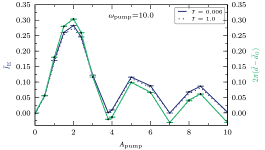

- a negative response of the the heat current due to probing

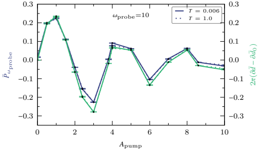

- control of effective temperature and dooouble occupation

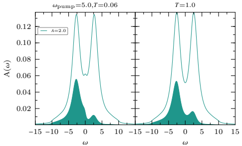

High-frequency expansion

start with time-evolution operator for a single period:

$$U(T+t_0,t_0) = \mathscr{T} e^{-i\int_{t_0}^{t_0+T} dt H(t)} = e^{-iH_F[t_0]T}$$

$$H_F[t_0] = \frac{i}{T} log[\mathscr{T} e^{-i\int_{t_0}^{t_0+T} dt H(t)}]$$

use Baker-Hausdorff lemma:

$$log(exp(X)exp(Y)) = X + Y + \frac{1}{2}[X,Y] + \ldots$$

Energy current

$$I_E(t) = \int_0^t d\tau \Delta_f^<(t,\tau) G^<(t,\tau)$$

$$\Delta_f^<(t,\tau) = \int_{-\infty}^{\infty} \frac{d\omega}{\pi} exp^{-i\omega(t-\tau)} \omega \Gamma(\omega) f(\omega-\mu)$$